Available online at www.sciencedirect.com
SCIENCE DIRECT®
Analytical Biochemistry 342 (2005) 292–299
ANALYTICAL BIOCHEMISTRY
www.elsevier.com/locate/yabio

Fluorescence and analytical ultracentrifugation analyses of the interaction of the tyrosine kinase inhibitor, tyrphostin AG1478-mesylate, with albumin

Andrew H.A. Clayton [a,1], Matthew A. Perugini [b,1], Janet Weinstock [a], Julie Rothacker [a], Keith G. Watson [c], Antony W. Burgess [a], Edouard C. Nice [a,*]

[a] *Ludwig Institute for Cancer Research, Melbourne Tumour Biology Branch, P.O. Royal Melbourne Hospital, Parkville, Vic. 3050, Australia*
[b] *Russell Grimwade School of Biochemistry and Molecular Biology, University of Melbourne, and Bio21 Molecular Science and Biotechnology Institute, Parkville, Vic. 3010, Australia*
[c] *Walter and Eliza Hall Institute for Medical Research, P.O. Royal Melbourne Hospital, Parkville, Vic. 3050, Australia*

Received 17 February 2005
Available online 22 April 2005

Abstract

Quantifying the interaction of drugs with carrier proteins in plasma is of importance for understanding effective drug delivery to disease-affected tissues. In this study, we employed analytical ultracentrifugation and steady-state fluorescence spectroscopy to characterize the interaction of a potential new anticancer drug, AG1478-mesylate, with plasma proteins in a suspension of normal serum albumin (NSA). We found that mesylate salt of AG1478, an epidermal growth factor receptor kinase inhibitor, sediments in 0.1%(w/v) NSA as a complex with a sedimentation coefficient of 3.8 S. This is consistent with the size of human serum albumin. This interaction was quantitated by meniscus depletion sedimentation and fluorescence titration analyses. AG1478-mesylate binds to albumin with an apparent single-site affinity (K_d) of 120 μM. In this article, we show that the cyclodextrin carrier molecule, Captisol, increases the apparent affinity of the hydrophobic AG1478-mesylate for albumin ($K_d = 4$–6 μM), and we propose that the AG1478-mesylate–Captisol (1:1) complex binds to albumin with at least 10-fold higher affinity than does AG1478-mesylate ligand alone. A fluorenylmethoxycarbonyl–sulfonic acid (FMS) derivative of the 6-aminoquinazoline analog of AG1478, which was designed to have improved serum-binding properties, was shown by fluorescence analysis to bind with approximately 100-fold greater affinity than the parent compound. This has significant implications in the effective delivery of therapeutic agents in vivo.

Keywords: Analytical ultracentrifugation; Fluorescence; Drug binding; Tyrphostin; AG1478; Tyrosine kinase inhibitor

The interaction of drugs with plasma proteins affects drug bioavailability and pharmacokinetics and can have a major influence on pharmacological activity [1,2]. Human serum albumin (HSA)[2] is the most abundant plasma protein, accounting for approximately 60% of the total protein with a concentration of roughly 40 mg/ml (0.6 mM) [2]. The chief physiological role of albumin is the transport of nonesterified fatty acids in the extracellular fluid. However, albumin also binds and transports a wide range of other endogenous substances,

* Corresponding author. Fax: +61 3 9341 3104.
E-mail address: ed.nice@ludwig.edu.au (E.C. Nice).
[1] These two authors contributed equally to this work.
[2] *Abbreviations used:* HSA, human serum albumin; ADME, absorption, distribution, metabolism, and excretion; EGFR, epidermal growth factor receptor; AG1478, tyrphostin 4-(3-chloroanilino)-6,7-dimethoxyquinazoline; NSA, normal serum albumin; RP, reversed-phase; ESI, electrospray ionization; RMSD, root mean square deviation.

0003-2697/$ - see front matter © 2005 Elsevier Inc. All rights reserved.
doi:10.1016/j.ab.2005.04.002

including bilirubin, bile salts, steroid hormones, hematin, tryptophan, thyroxine, and some vitamins and metal ions [1,2]. It has also been suggested that albumin has a buffering function in blood that contributes to the maintenance of pH [1,2].

Because of the high circulating plasma levels and the capacity of albumin to bind a diverse range of compounds, it is generally assumed that the drug–albumin interaction is the dominant one. Determining a drug candidate's propensity for binding albumin is, therefore, a major goal of preclinical ADME (absorption, distribution, metabolism, and excretion) studies [3]. It is interesting to note that a large proportion of drugs with good biological activity fail to progress to later stages of drug development due to poor pharmacokinetics and pharmacodynamics [4]. However, binding to albumin can also be advantageous because this can help to solubilize hydrophobic drugs [2], and the increase in apparent size helps to prevent metabolic clearance and, hence, increase the lifetime [2,5]. Measuring drug–albumin interactions is, therefore, an area of intense research interest. Methods of assessing or quantifying such interactions include microdialysis [6], electrophoresis [7], LC–MS [8], high-performance affinity chromatography [9,10], ultracentrifugation [11], surface-enhanced Raman spectroscopy [12], UV and fluorescence spectroscopy [13], and optical biosensor detection [14–17].

Dysregulation of the epidermal growth factor receptor (EGFR) family is associated with a large number of epithelial cancers [18,19]. This signaling pathway has, therefore, become a major target for drug discovery [19]. The tyrphostin 4-(3-chloroanilino)-6,7-dimethoxyquinazoline (AG1478, Fig. 1A), which is a competitive inhibitor of the ATP binding site in the EGFR kinase domain [20,21], is a highly potent and specific small molecule inhibitor of EGFR (ErbB1) tyrosine kinase [22] and is a potential new anticancer agent [23–25]. However, AG1478 is very hydrophobic and shows poor aqueous solubility, particularly at physiological salt concentrations. Attempts to measure the interaction of AG1478 with plasma proteins using standard ultrafiltration methods have yielded inconsistent results due to absorption of AG1478 onto the filter membrane (E. Nice, unpublished results). Here, we show two alternative approaches: (i) sedimentation meniscus depletion studies using the analytical ultracentrifuge, which directly measures free and/or bound ligand, and (ii) equilibrium fluorescence titration, which measures the increase in the ligand fluorescence quantum yield on binding to plasma proteins. We applied these methods to study the binding of the mesylate salt of AG1478 (hereafter referred to as AG1478-mesylate) to a suspension of serum proteins and examined the effect of a carrier cyclodextrin, Captisol, and fluorenylmethoxycarbonyl–sulfonic acid (FMS) derivatization of the 6-aminoquinazoline analog of AG1478 (Fig. 1B) on the drug–plasma protein interaction.

Materials and methods

AG1478-mesylate/Captisol (49 mM AG1478-mesylate and 49 mM Captisol in water) was obtained from the Ludwig Institute for Cancer Research Biological Production Facility (Austin Hospital, Heidelberg, Victoria, Australia). Normal serum albumin (NSA), a 20%(w/v) human albumin preparation for intravenous administration from pooled human plasma prepared by ethanol fractionation and chromatography, was obtained from CSL Limited (Broadmeadows, Victoria, Australia).

The 6-amino-4-(3-chlorophenylamino) quinazoline was prepared as described previously [22], and 9-fluorenylmethoxycarbonylchloride-2-sulfonic acid (FMS–Cl) was prepared as reported by Merrifield and Bach [26].

Synthesis of the FMS-6-aminoquinazoline derivative of AG1478

The FMS-6-aminoquinazoline derivative was synthesized as follows. A suspension of 6-amino-4-(3-chlorophenylamino) quinazoline (270 mg, 1.0 mmol), 9-fluorenylmethoxycarbonylchloride-2-sulfonic acid (340 mg, 1.0 mmol), and potassium acetate (150 mg, 1.5 mmol) in ethyl acetate (15 ml) was stirred gently at room temperature under a drying tube for 48 days (the FMS derivative was found to form very slowly, but cleanly, at room temperature. Reaction at room temperature for 2 days gave incomplete conversion (15% yield) with recovery of much starting 6-amino compound). The reaction mixture was poured into a separating funnel,

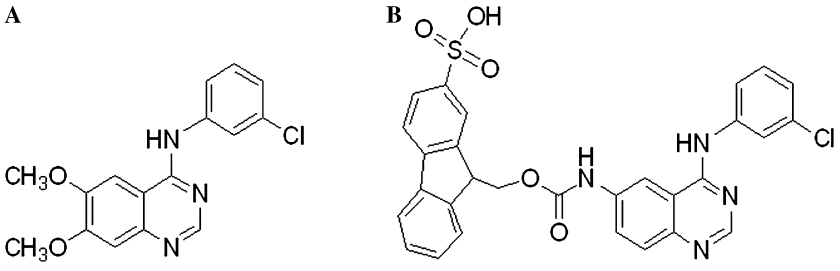

Fig. 1. Chemical structures of the tyrphostin AG1478 (A) and the FMS-6-aminoquinazoline derivative (B).

followed by the addition of extra ethyl acetate (100 ml) and then ice water (100 ml). The mixture was shaken vigorously for several minutes, the suspension was filtered to give a pale olive solid that was washed with additional ice water (50 ml) and ethyl acetate (50 ml), and then the solid was dried in a vacuum oven to give the crude product as an olive-colored solid (420 mg, 73%), ^{1}H NMR spectrum (d_6DMSO): δ 4.35 (m, 1H), 4.64 and 4.79 (each dd, 1H), 7.33–7.90 (complex m, 15H), 8.06 (s, 1H), 8.72 (s, 1H), 8.85 (s, 1H), 10.19 (s, 1H), 11.50 (bs, 1H).

Reversed-phase HPLC purification of the FMS-6-aminoquinazoline derivative of AG1478

The FMS-6-aminoquinazoline derivative of AG1478 was separated from unreacted 6-amino-4-(3-chlorophenylamino)quinazoline by reversed-phase (RP)–HPLC [27]. All separations were performed using an Agilent model 1100 HPLC (Agilent Technologies, Victoria, Australia) equipped with a diode array detector and using a Brownlee Aquapore RP-300 (Octyl C8) 7-μm 100 × 2.1-mm column. Separation was achieved by gradient elution using a linear 40-min gradient between 10 mM ammonium acetate (pH 6.0) and 100% acetonitrile. The flow rate was 0.1 ml/min, and the column temperature was 25 °C. Detection was at 330 nm. Fractions were recovered manually, with allowance being made for the dead volume between the detector and trapping port. Electrospray ionization (ESI)–MS analysis of the purified material, which had a characteristic retention time of 23.9 min, gave the anticipated mass of 573.2 $(M + H)^+$.

Analytical ultracentrifugation

Sedimentation experiments were conducted in a Beckman model XL-A analytical ultracentrifuge at a temperature of 20 °C. Samples of AG1478-mesylate (2.5, 5, 10, 20, and 40 μM complexed with 1:1 Captisol), NSA (0.1%, w/v), and mixtures of both dissolved in ddH_2O were loaded into a conventional double sector quartz cell and mounted in a Beckman four-hole An-60 Ti rotor. Then 300 μl of sample and 320 μl of reference solution were centrifuged at a rotor speed of 40,000 rpm, and the data were collected for 4 h at 340 nm in continuous mode using a time interval of 300 s and a step size of 0.003 cm without averaging. A wavelength of 340 nm was selected to monitor the progression of sedimentation because AG1478-mesylate absorbs strongly at this wavelength, whereas the acceptor (0.1% NSA) contributes to only minor near-baseline absorbance signals at this wavelength. To determine the signal due to free AG1478-mesylate, a method adapted from Perugini et al. [28] was employed. In brief, the absorbance due to free ligand was averaged over a radial range of 0.1 cm in the plateau region adjacent to the sample meniscus at 4 h postcentrifugation. At this time point, the signal due to bound AG1478-mesylate was at the bottom of the cell. The absorbance signal of free ligand was converted to concentration units (μM) using a four-point standard curve, and from this a binding isotherm was constructed. Nonlinear least squares analyses of the binding data to a number of different models, including single-site binding and independent two-site binding, were implemented using the program SigmaPlot. To estimate the sedimentation coefficient distribution of the bound AG1478-mesylate–NSA protein complex, ls–$g^*(s)$ analyses [29] were performed with mixtures of AG1478-mesylate complexed with Captisol (1:1 molar ratio) and 0.1% NSA using the program SEDFIT [29] (available at www.analyticalultracentrifugation.com).

Fluorescence spectroscopy

The binding of the AG1478-mesylate to NSA was determined by the increase in quantum yield of AG1478-mesylate fluorescence. Fluorescence titrations were conducted with a SPEX FluoroLog tau-2 frequency domain spectrofluorometer operated in the steady-state mode at a temperature of 20 °C. AG1478-mesylate was excited with vertically polarized emissions from a xenon lamp at a wavelength of 350 nm. AG1478-mesylate emissions were collected at the magic angle polarization (54.7°) at 400 nm. Quartz cuvettes containing a fixed concentration of AG1478-mesylate (10 or 50 μM in 1:1 Captisol or 10 μM in distilled water) were titrated with variable amounts of NSA. Background scatter and background fluorescence were corrected for using blank samples containing only NSA. The fluorescence data were analyzed to either a single-site or two-site model using nonlinear least squares fitting (Microsoft Excel and Prism). For single-site binding, the emission intensity (y) as a function of added NSA was fit to the function $y = (A/2/D)^*[C + X + D - \mathrm{SQRT}((C + X + D)^2 - 4XD)]$, where A = change in intensity at saturation, B = initial intensity, $C = K_d$, D = concentration of AG1478 (fixed), and X = concentration of NSA. The change in intensity at saturation was either used as a fitting parameter (in cases where obvious saturation was observed) or extrapolated using a double reciprocal plot.

Results

Analytical ultracentrifugation

To estimate the propensity of AG1478-mesylate to bind to plasma proteins in a suspension of 0.1% NSA, sedimentation velocity studies were performed in the analytical ultracentrifuge. Data were obtained with 2.5, 5, 10, 20, and 40 μM AG1478-mesylate. For all samples analyzed, the absorbance versus radial profiles plotted as a function of time indicated that a significant proportion

of the ligand was sedimenting with a larger macromolecule in the sample solution. As an example, the absorbance at 340 nm versus radial position profiles for 40 μM AG1478-mesylate + 0.1% NSA are shown at 12-min intervals in Fig. 2A. These data were fitted by nonlinear least squares ls–$g^*(s)$ analysis to yield the sedimentation coefficient distribution shown in Fig. 2B. The low root mean square deviation (RMSD) of 0.0093 and random distribution of residuals (Fig. 2A, inset) demonstrate an excellent fit to the data. The ls–$g^*(s)$ distribution shows that AG1478-mesylate is largely bound to a species with a sedimentation coefficient of approximately 3.8 S, which is consistent with the sedimentation coefficient of monomeric albumin reported by Squire et al. [30]. Furthermore, the material observed in the ls–$g^*(s)$ distribution at $s \sim 7$ S may indicate a small amount of AG1478-mesylate bound to the albumin dimer (Fig. 2B). Together, these data suggest that a significant proportion of the ligand binds human albumin in the NSA suspension.

To further quantitate the interaction of AG1478-mesylate with albumin, the sedimentation data obtained with 2.5–40 μM AG1478-mesylate and a fixed concentration of 0.1% NSA were analyzed further. As shown in Fig. 2A, there is a significant nonzero absorbance ($Abs_{340\,nm} \sim 0.29$) at the top of the cell at radial positions of approximately 6.4–6.6 cm, particularly at the latter time points of the experiment. This baseline offset represents the absorbance of free AG1478-mesylate. It is also indicated by the steep increase in ls-$g^*(s)$ as the sedimentation coefficient distribution decreases from 2.0 S to less than 0.5 S (Fig. 2B). At each of the five AG1478-mesylate concentrations employed (2.5, 5, 10, 20, and 40 μM), the baseline offset was converted to concentration units using the four-point standard curve shown in the Fig. 3 inset, and the proportion of free ligand was calculated directly. This allowed the binding isotherm shown in Fig. 3 to be constructed. The data in this figure were fitted to various models. A single-site binding model yielded an apparent K_d of 3.5 μM ($R = 0.984$). However, the nonlinear least squares best fit ($R = 0.996$) obtained was an

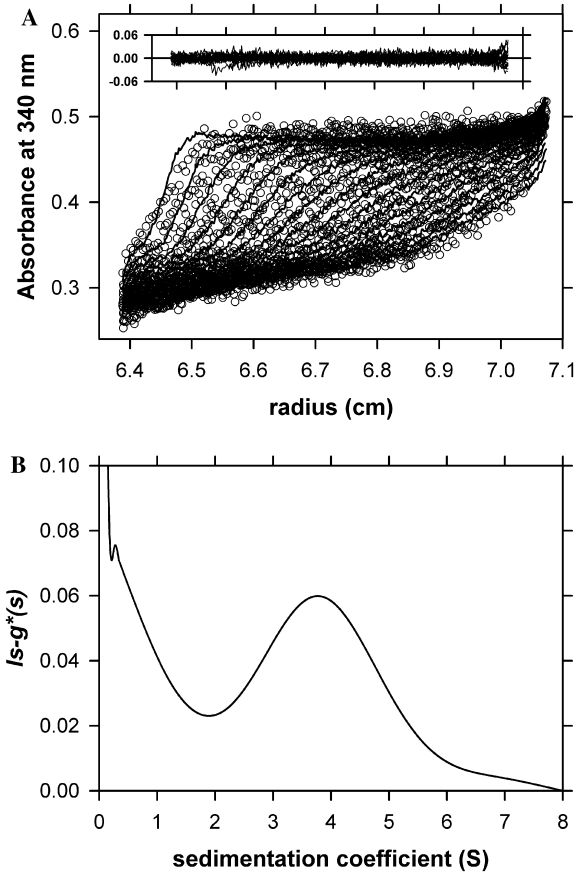

Fig. 2. Area under the curve sedimentation velocity analysis of bound AG1478-mesylate. (A) The absorbance at 340 nm is plotted as a function of radius (cm) at 12-min intervals. The raw absorbance data (symbols) is overlaid with the nonlinear least squares $g^*(s)$ [ls–$g^*(s)$] best fits (solid lines) [29]. Sedimentation velocity experiments of AG1478-mesylate (40 μM) in the presence of 0.1%(w/v) NSA were conducted in a Beckman model XL-A analytical ultracentrifuge as described in Materials and methods. (B) ls-$g^*(s)$ distribution plotted as a function of sedimentation coefficient (S). Analysis was performed using the program SEDFIT with 100 sedimentation coefficients between 0.5 and 8.0 S and at a confidence level of 0.95.

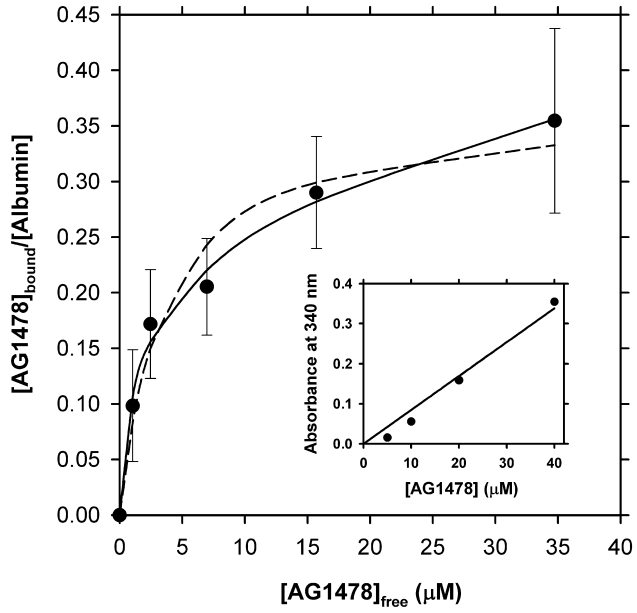

Fig. 3. Binding isotherm of AG1478-mesylate to human albumin in 0.1% NSA derived from area under the curve data. The amount of bound AG1478-mesylate ligand divided by the total human albumin concentration (14.8 μM) is plotted as a function of free AG1478-mesylate. The data (solid circles) were fitted to a single-site binding model that yielded a $K_d = 3.6$ (dashed line) and an independent two-site binding model (solid line) that yielded a nonlinear best fit (solid line) with $K_{d1} = 1.0$ μM ($n_1 = 0.19$) and $K_{d2} = 42$ μM ($n_2 = 0.38$). The multiple correlation coefficients (R) of the nonlinear best fits shown were calculated to be 0.984 for the one-site model and 0.996 for the two-site model. The inset shows a four-point standard curve used to convert the absorbance at 340 nm in the supernatant to the amount of free AG1478-mesylate (μM) as described in Materials and methods and as adapted from [28].

independent two-site model with $K_{d1} = 1.0\,\mu M$ ($n_1 = 0.19$) and $K_{d2} = 42\,\mu M$ ($n_2 = 0.38$). This suggests that AG1478-mesylate could bind to at least two different sites on the albumin monomer.

Fluorescence spectroscopy

To provide a further probe of the AG1478-mesylate–NSA interaction and to confirm the analytical ultracentrifugation results, experiments were carried out using the environmentally sensitive fluorescence from the AG1478-mesylate. Fig. 4A illustrates a titration of variable amounts of NSA with a fixed (10 μM) concentration of AG1478-mesylate and Captisol. The AG1478-mesylate undergoes a large (>10-fold) increase in fluorescence as the NSA is added, indicative of an interaction between AG1478-mesylate and one or more components of NSA. The large enhancement indicates that the fluorescence measurements are particularly sensitive and weighted toward the bound form of AG1478-mesylate. Similar data, but with a starting concentration of 50 μM AG1478-mesylate and Captisol, are shown for comparison in Fig. 4B. The data in Fig. 4A were fitted to various models for the AG1478-mesylate–NSA interaction. A fit to a single-site model yielded a K_d of 5.5 μM for a 1:1 stoichiometry ($R = 0.99$). To compare with the analytical ultracentrifuge data, we transformed the data in Fig. 4A to a percentage bound versus free HSA concentration plot. The nonlinear least squares best fit was obtained to an independent two-site model with $K_{d1} = 1.7\,\mu M$ ($n_1 = 0.43$) and $K_{d2} = 16.7\,\mu M$ ($n_2 = 0.59$) ($R = 0.99$), which was statistically more significant than that obtained to the one-site model ($R = 0.98$). This is in good agreement with the analytical ultracentrifugation data described in Fig. 3.

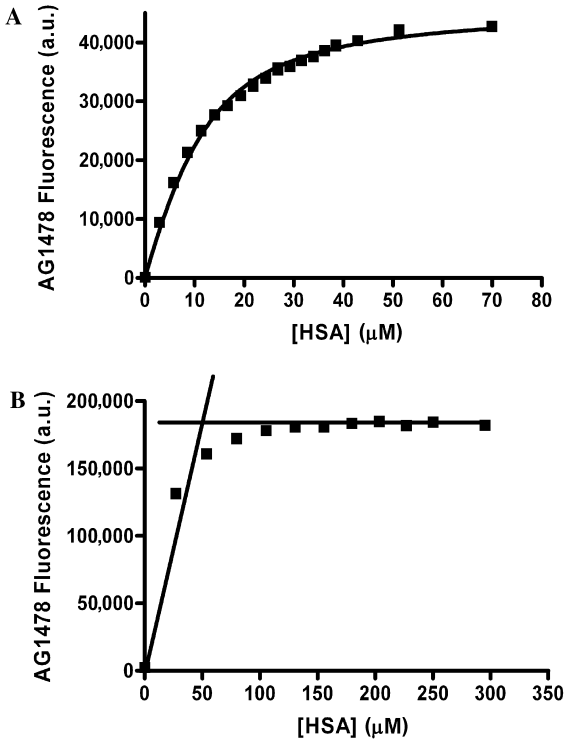

Fig. 4. Fluorescence titration of AG1478-mesylate with NSA. The plot shows the AG1478-mesylate fluorescence as a function of added NSA (as equivalent HSA concentration). (A) 10 μM AG1478-mesylate:10 μM Captisol. (B) 50 μM AG1478-mesylate:50 μM Captisol. Solid squares represent the measured data points. Solid lines represent the fit to an interaction with a K_d of 6 μM (A) and a binding curve extrapolation (B) for a 1:1 interaction. a.u., arbitrary units.

To assess the influence of the added Captisol on the AG1478-mesylate–NSA interaction, we performed a titration of NSA with AG1478-mesylate in the absence of Captisol and a separate titration of AG1478-mesylate with Captisol in the absence of NSA. The limited solubility of AG1478-mesylate in the absence of Captisol (soluble up to 100 μM in ddH_2O) prevented titrations from being carried out at concentrations of AG1478-mesylate greater than 100 μM. Fig. 5 illustrates a titration of variable amounts of NSA with a fixed 10-μM concentration of AG1478-mesylate in the absence of Captisol. The solid line depicts a fit to a single-site model with a K_d of 190 μM. Duplicate measurements yielded a mean K_d of 120 μM. It is apparent that the Captisol has a marked effect on the distribution of free and bound AG1478-mesylate.

A titration of 50 μM AG1478-mesylate with Captisol produced a relatively mild fluorescence enhancement (approximately twofold increase) in comparison with NSA and showed stoichiometric binding with a stoichiometry of 1:1. Based on these results and the comparative titrations with NSA, we estimate that the K_d for the Captisol–AG1478-mesylate interaction is approximately 5 μM. We also studied the AG1478-mesylate–Captisol complex in the analytical ultracentrifuge to determine the apparent molar mass at a 1:1 molar ratio. At 40-μM starting concentrations for both AG1478-mesylate ($M_r = 315.8$ g/mol) and Captisol ($M_r \sim 2179$ g/mol), the

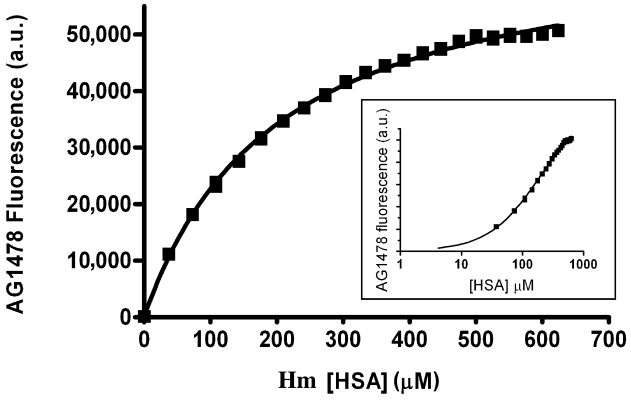

Fig. 5. Fluorescence titration of AG1478-mesylate with NSA in the absence of Captisol. The plot shows the AG1478-mesylate fluorescence as a function of added NSA (as equivalent HSA concentration) (10 μM AG1478-mesylate in distilled water). Solid squares represent the measured data points. The solid line represents the fit to a 1:1 interaction with a K_d of 190 μM. The inset shows a plot with log scale on the concentration axis. a.u., arbitrary units.

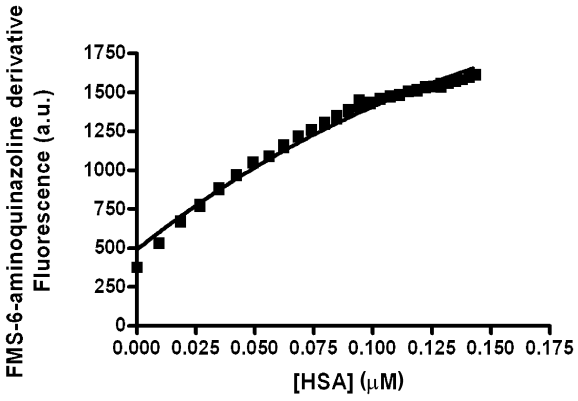

Fig. 6. Fluorescence titration of a FMS-6-aminoquinazole derivative with NSA in the absence of Captisol. The plot shows FMS-6-aminoquinazole fluorescence as a function of added NSA (as equivalent HSA concentration) in the presence of 0.1 μM FMS-6-aminoquinazole derivative in distilled water. Solid squares represent the data points. The solid line represents a fit to a 1:1 interaction with a K_d of 0.1 μM. a.u., arbitrary units.

apparent molar mass assuming a single species was calculated to be 1640 g/mol by sedimentation equilibrium analysis. This indicates that a significant amount of AG1478-mesylate is bound to Captisol under these conditions, consistent with the fluorescence titration data. Fig. 6 shows a preliminary fluorescence titration for a candidate prodrug FMS derivative (Fig. 1B) binding to NSA. The affinity for this interaction is estimated to be 0.1 μM. The parent 6-amino quinazoline compound (lacking the FMS group) binds with an affinity of 170 μM. Experiments with Captisol were not attempted with this FMS derivative due to its high water solubility and high affinity for NSA in the absence of Captisol.

Discussion

The two complementary approaches used in the current investigation clearly show that AG1478-mesylate binds to HSA with an apparent single-site affinity (K_d) of approximately 100 μM, which increases by a factor of more than 10 in the presence of the carrier β-cyclodextrin, Captisol ($K_d = 4–6$ μM). Captisol has been shown to improve the aqueous solubility of hydrophobic drugs [31–36]. Although the entire cyclodextrin molecule is water soluble, the interior of the molecule is relatively apolar and creates a hydrophobic microenvironment with the ability to encapsulate hydrophobic water-insoluble molecules [36]. This has permitted aqueous formulations of high AG1478 concentration (>90 mM) for the xenograft studies and the assessment of tissue distribution and pharmacokinetics of AG1478 in mice and rats [24]. Although our study used a preparation of serum albumin (20% NSA) that may contain traces of other proteins and serum electrolytes, the sedimentation velocity analysis showed that the sedimentation coefficient of bound AG1478-mesylate (3.8 S) was consistent with that of albumin (Fig. 1B). Given this, an important question to address here is how the binding of AG1478-mesylate to human albumin compares with other drugs and ligands. We make a comparison below with fatty acids in accordance with albumin's primary physiological role as a fatty acid binder [1,2]. In addition, we compare our data set with thyroxin–albumin interaction (which occurs in plasma) and a panel of hydrophobic drugs.

Loun and Hage [10] used high-performance affinity chromatography containing immobilized HSA to study the binding of thyroxine at the warfarin and indole sites of HSA. Frontal analysis, using *R*-warfarin and L-tryptophan as probes for these sites, demonstrated that the immobilized HSA had binding behavior equivalent to that observed for HSA in solution. The warfarin and indole sites had relatively strong binding for thyroxine, with dissociation constants of 7.1 and 1.8 μM, respectively [10], in the range observed for AG1478-mesylate in the current study.

In contrast, the analysis of fatty acid binding to albumin requires multisite models [2,37]. Crystal structures (for reviews, see [2,38,39]) have shown that albumin is a three-lobed, heart-shaped molecule with approximate dimensions of $80 \times 80 \times 30$ Å. On binding to fatty acids, a large conformational change occurs. Binding involves a number of structurally distinct sites with varying affinities [38]. In a study using equilibrium dialysis [37], Scatchard analysis indicated two classes of binding sites, with the first class having $n_1 = 4.2–5.0$ sites and the second class having $n_2 = 27–31$ sites. The dissociation constants decreased as the chain length of the fatty acids increased; that is, K_{d1} was 12.5 mM for acetate, 1.8 mM for hexanoate, and 0.15 mM for octanoate. Thus, the longer chain fatty acids would appear to have more similar affinity for albumin than for AG1478-mesylate.

More recently, the group of Caron and co-workers [11] compared the binding of 14 different drugs to albumin and attempted to correlate the fraction bound with ionization and lipophilicity descriptors. Under the conditions of their ultracentrifugation assay (600 μM albumin, drug concentration 20 μM), 3 of the drugs (acebutolol, chloroquine, and ranitidine) showed little binding (<10% bound), whereas the binding of the remaining 11 drugs varied from 27.8% to more than 95.0%. It is clear from our fluorescence study (Figs. 4 and 5) that at physiological concentrations of albumin, 10 μM AG1478-mesylate in the presence or absence of Captisol is mostly albumin bound. To compare directly with Caron and co-workers' study [11], we would predict, on the basis of $K_d = 120$ μM, that approximately 90% of 20 μM AG1478-mesylate is bound to albumin.

The most striking observation from the current work is that the carrier cyclodextrin, Captisol, appears to enhance the affinity of the AG1478-mesylate for the plasma proteins. This enhancement cannot be reconciled with com-

petitive displacement from the AG1478-mesylate–cyclodextrin complex or drug release by simple dilution because the first effect would reduce the apparent affinity and the second effect would have no consequence. Moreover, the analytical ultracentrifugation clearly shows that AG1478-mesylate sediments with albumin in the presence of Captisol (Fig. 2). The current data suggest that the K_d for the cyclodextrin–AG1478-mesylate complex provided by fluorescence titration data is not greater than 5 μM given that stoichiometric binding behavior is observed at an AG1478-mesylate concentration of 50 μM. In general, stoichiometric binding becomes evident at concentrations 10-fold higher than the K_d for the interaction [40]. Compared with other cyclodextrin–drug complexes [32,33], the affinity constant for AG1478-mesylate–Captisol is in the upper range, on the order of 10 μM. Under the experimental conditions of 10 μM AG1478-mesylate and 10 μM Captisol, a significant fraction of AG1478-mesylate will be bound to Captisol as an AG1478-mesylate–cyclodextrin complex. Based on the fluorescence and sedimentation data, it seems reasonable to propose that the AG1478-mesylate forms a ternary or higher order complex with both cyclodextrin and albumin.

We are currently using these methods to aid in the development of AG1478 derivatives with improved binding to plasma and, therefore, prolonged half-lives in vivo (Fig. 1B). The 6-amino quinazoline parent compound (i.e., lacking the FMS group) has similar binding affinity ($K_d = 170$ μM) for NSA as for AG1478-mesylate in the absence of Captisol ($K_d = 120$ μM). However, the FMS derivative binds more than 1000-fold more tightly than the parent compound ($K_d = 0.1$ μM). This is in line with previous reports showing enhanced binding and extended plasma half-lives of other drugs conjugated to fluorenylmethoxycarbonyl [41,42]. Although the FMS derivative has significantly reduced biological activity, it is readily hydrolyzed to yield a biologically active form with an IC_{50} similar to that of the parent AG1478. Work is in progress to characterize the biological pharmokinetics of this drug and to determine its efficacy as a new tyrosine kinase inhibitor.

In summary, we have shown a drug fluorescence-based approach to plasma protein binding that is fast, sensitive, and nondestructive and that could be easily adapted to plate-reader configurations.

Acknowledgments

We gratefully acknowledge the useful advice from and discussions with Mati Fridkin and Yoram Schecter of the Weizmann Institute of Science, Rehovot, Israel. Andrew H. A. Clayton is the recipient of an R.D. Wright Biomedical Career Development Award from the Australian National Health and Medical Research Council (NHMRC). This work was also supported by the Australian NHMRC Project (grants 164809, 234709, and 280918 and program grant 280912).

References

[1] G. Colmenarejo, In silico prediction of drug-binding strengths to human serum albumin, Med. Res. Rev. 23 (2003) 275–301.
[2] C. Bertucci, E. Domenici, Reversible and covalent binding of drugs to human serum albumin: methodological approaches and physiological relevance, Curr. Med. Chem. 9 (2002) 1463–1481.
[3] Y.S. Day, D.G. Myszka, Characterizing a drug's primary binding site on albumin, J. Pharm. Sci. 92 (2003) 333–343.
[4] R.A. Prentis, Y. Lis, S.R. Walker, Pharmaceutical innovation by seven U.K.-owned pharmaceutical companies (1964–1985), Br. J. Clin. Pharmacol. 25 (1988) 387–396.
[5] S. Rahimipour, N. Ben-Aroya, M. Fridkin, Y. Koch, Design, synthesis, and evaluation of a long-acting, potent analogue of gonadotropin-releasing hormone, J. Med. Chem. 44 (2001) 3645–3652.
[6] Y. Huang, Z. Zhang, Binding study of drug with bovine serum albumin using a combined technique of microdialysis with flow-injection chemiluminescent detection, J. Pharm. Biomed. Anal. 35 (2004) 1293–1299.
[7] J. Ostergaard, C. Schou, C. Larsen, N.H. Heegaard, Evalution of capillary electrophoresis–frontal analysis for the study of low molecular weight drug–human serum albumin interactions, Electrophoresis 23 (2002) 2842–2853.
[8] Y. Cheng, E. Ho, B. Subramanyam, J.L. Tseng, Measurements of drug–protein binding by using immobilized human serum albumin liquid chromatography–mass spectrometry, J. Chromatogr. B Anal. Technol. Biomed. Life Sci. 809 (2004) 67–73.
[9] J. Chen, C. Ohnmacht, D.S. Hage, Studies of phenytoin binding to human serum albumin by high-performance affinity chromatography, J. Chromatogr. B Anal. Technol. Biomed. Life Sci. 25 (2004) 137–145.
[10] B. Loun, D.S. Hage, Characterization of thyroxine–albumin binding using high-performance affinity chromatography: I. Interactions at the warfarin and indole sites of albumin, J. Chromatogr. 579 (1992) 225–235.
[11] G. Ermondi, M. Lorenti, G. Caron, Contribution of ionization and lipophilicity to drug binding to albumin: a preliminary step toward biodistribution prediction, J. Med. Chem. 47 (2004) 3949–3961.
[12] G. Fabriciova, S. Sanchez-Cortes, J.V. Garcia-Ramos, P. Miskovsky, Surface-enhanced Raman spectroscopy study of the interaction of the antitumoral drug emodin with human serum albumin, Biopolymers 74 (2004) 125–130.
[13] J. Seetharamappa, B.P. Kamat, Spectroscopic studies on the mode of interaction of an anticancer drug with bovine serum albumin, Chem. Pharm. Bull. (Tokyo) 52 (2004) 1053–1057.
[14] C. Bertucci, S. Cimitan, Rapid screening of small ligand affinity to human serum albumin by an optical biosensor, J. Pharm. Biomed. Anal. 8 (2003) 707–714.
[15] A. Frostell-Karlsson, A. Remaeus, H. Roos, K. Andersson, P. Borg, M. Hamalainen, R. Karlsson, Biosensor analysis of the interaction between immobilized human serum albumin and drug compounds for prediction of human serum albumin binding levels, J. Med. Chem. 43 (2000) 1986–1992.
[16] R.L. Rich, Y.S. Day, T.A. Morton, D.G. Myszka, High-resolution and high-throughput protocols for measuring drug/human serum albumin interactions using BIACORE, Anal. Biochem. 296 (2001) 197–207.
[17] A. Ahmad, A. Ramakrishnan, M.A. McLean, A.P. Breau, Use of surface plasmon resonance biosensor technology as a possible alternative to detect differences in binding of enantiomeric drug compounds to immobilized albumins, Biosens. Bioelectron. 18 (2003) 399–404.

[18] D.J. Riese II, D.F. Stern, Specificity within the EGF family/ErbB receptor family signaling network, Bioessays 20 (1998) 41–48.
[19] J. Baselga, Why the epidermal growth factor receptor? The rationale for cancer therapy, Oncologist 7 (Suppl. 4) (2002) 2–8.
[20] A. Levitzki, Protein kinase inhibitors as a therapeutic modality, Accounts Chem. Res. 2003 (2003) 462–469.
[21] R.B. Lichtner, A. Menrad, A. Sommer, U. Klar, M.R. Schneider, Signaling-inactive epidermal growth factor receptor/ligand complexes in intact carcinoma cells by quinazoline tyrosine kinase inhibitors, Cancer Res. 61 (2001) 5790–5795.
[22] T.J. Powell, H. Ben-Bassat, B.Y. Klein, H. Chen, N. Shenoy, J. McCollough, B. Narog, A. Gazit, Z. Hartzstark, M. Chaouat, R. Levitzki, C. Tang, J. McMahon, L. Shawer, A. Levitzki, Growth inhibition of psoriatic keratinocytes by quinazoline tyrosine kinase inhibitors, Br. J. Dermatol. 141 (1999) 802–810.
[23] A. Levitzki, A. Gazit, Tyrosine kinase inhibition: an approach to drug development, Science 267 (1995) 1782–1788.
[24] T.G. Johns, R.B. Luwor, C. Murone, F. Walker, J. Weinstock, A.A. Vitali, R.M. Perera, A.A. Jungbluth, E. Stockert, L.J. Old, E.C. Nice, A.W. Burgess, A.M. Scott, Antitumor efficacy of cytotoxic drugs and the monoclonal antibody 806 is enhanced by the EGF receptor inhibitor AG1478, Proc. Natl. Acad. Sci. USA 100 (2003) 15871–15876.
[25] H-R. Tsou, N. Mamuya, B.D. Johnson, M.F. Reich, B.C. Gruber, F. Ye, R. Nilakantan, R. Shen, C. Discafani, R. DeBlanc, R. Davis, F.E. Koehn, L.M. Greenberger, Y.-F. Wang, A. Wissner, 6-Substituted-4-(3-bromophenylamino)quinazolines as putative irreversible inhibitors of the epidermal growth factor receptor (EGFR) and human epidermal growth factor receptor (HER-2) tyrosine kinases with enhanced antitumor activity, J. Med. Chem. 44 (2001) 2719–2734.
[26] R.B. Merrifield, A.E. Bach, 9-(2-Sulfo)fluorenylmethyloxycarbonyl chloride, a new reagent for the purification of synthetic peptides, J. Org. Chem. 43 (1978) 4808–4816.
[27] A.G. Ellis, E.C. Nice, J. Weinstock, A. Levitzki, A.W. Burgess, L.K. Webster, High-performance liquid chromatographic analysis of the tyrphostin AG1478-mesylate, a specific inhibitor of the epidermal growth factor receptor tyrosine kinase, in mouse plasma, J. Chromatogr. B Biomed. Sci. Appl. 754 (2001) 193–199.
[28] M.A. Perugini, P. Schuck, G.J. Howlett, Differences in the binding capacity of human apolipoprotein E3 and E4 to size-fractionated lipid emulsions, Eur. J. Biochem. 269 (2002) 5939–5949.
[29] P. Schuck, P. Rossmanith, Determination of the sedimentation coefficient distribution by least-squares boundary modeling, Biopolymers 54 (2000) 328–341.
[30] P.G. Squire, P. Moser, C.T. O'Konski, The hydrodynamic properties of bovine serum albumin monomer and dimmer, Biochemistry 7 (1968) 4261–4272.
[31] V.J. Stella, R.A. Rajewski, Cyclodextrins: their future in drug formulation and delivery, Pharm. Res. 14 (1997) 556–567.
[32] V.J. Stella, V.M. Rao, E.A. Zannou, V. Zia, Mechanisms of drug release from cyclodextrin complexes, Adv. Drug Del. Rev. 36 (1999) 3–16.
[33] K. Okimoto, R.A. Rajewski, K. Uekama, J.A. Jona, V.J. Stella, The interaction of charged and uncharged drugs with neutral (HP-β-CD) and anionically charged (SBE7-β-CD) beta-cyclodextrins, Pharm. Res. 13 (1996) 256–264.
[34] H. Ueda, D. Ou, T. Endo, H. Nagase, K. Tomono, T. Nagai, Evaluation of a sulfobutyl ether beta-cyclodextrin as a solubilizing/stabilizing agent for several drugs, Drug Dev. Ind. Pharm. 24 (1998) 863–867.
[35] T. Loftsson, M.E. Brewster, Pharmaceutical applications of cyclodextrins: I. Drug solubilization and stabilization, J. Pharm. Sci. 85 (1996) 1017–1027.
[36] M.E. Davis, M.E. Brewster, Cyclodextrin-based pharmaceutics: past, present, and future, Nat. Rev. Drug Disc. 3 (2004) 1023–1035.
[37] A.A. Spector, Fatty acid binding to plasma albumin, J. Lipid Res. 16 (1975) 165–179.
[38] S. Curry, P. Brick, N.P. Franks, Fatty acid binding to human serum albumin: new insights from crystallographic studies, Biochim. Biophys. Acta 1441 (1999) 131–140.
[39] J.A. Hamilton, Fatty acid interactions with proteins: what X-ray crystal and NMR solution structures tell us, Prog. Lipid Res. 43 (2004) 177–199.
[40] D.J. Winzor, W.H. Sawyer, Quantitative Characterization of Ligand Binding, John Wiley, New York, 1995.
[41] Y. Shechter, L. Preciado-Patt, G. Schreiber, M. Fridkin, Prolonging the half-life of human interferon-alpha 2 in circulation: design, preparation, and analysis of (2-sulfo-9-fluorenylmethoxycarbonyl) 7-interferon-alpha 2, Proc. Natl. Acad. Sci. USA 98 (2001) 1212–1217.
[42] Y. Schechter, H. Tsubery, M. Fridkin, *N* -[(2-Sulfo)-9-fluorenylmethoxycarbonyl]-gentamycin C1 is a long-acting prodrug derivative, J. Med. Chem. 45 (2002) 4264–4270.